This is the Pre-Published Version.
The following publication Y. Zhang, X. Zhang and Z. Tang, "Lifetime Enhanced Modulation Method for Unbalanced Loss Issue in Sustainable Renewable Converters," in IEEE Transactions on Industrial Electronics, vol. 73, no. 6, pp. 8581-8590, June 2026 is available at https://doi.org/10.1109/TIE.2025.3637368.

Lifetime Enhanced Modulation Method for Unbalanced Loss Issue in Sustainable Renewable Converters

Yi Zhang, *Senior Member, IEEE*, Xinyue Zhang, *Member, IEEE*, and Zhongting Tang, *Member, IEEE*

***Abstract*—The increasing power losses in renewable energy converters can accelerate the degradation of power modules and reduce system reliability. This paper proposes an enhanced modulation method to address the unbalanced loss distribution in typical renewable converter modules. The approach periodically adjusts switching operation modes to equalize power losses and average the junction temperature of power devices. A full-bridge inverter module is used to demonstrate the method, and experiments confirm that it achieves a more balanced loss distribution compared with traditional modulation. Reliability analysis based on Weibull function-derived time-to-failure distributions and annual mission profiles of a 5 kW PV system in Arizona shows that the proposed method can significantly extend the lifetime of power modules without increasing system cost. Furthermore, life cycle assessment shows that the proposed method prevents at least two module replacements over a 25-year service life, reducing environmental impact. By improving module longevity, the method also contributes to the overall sustainability of renewable converters.**

***Index Terms*—Sustainable, lifetime, full-bridge inverter, hybrid PWM, loss unbalance, operating converters, life cycle assessment**

I. Introduction

POWER electronics are increasingly employed in various green energy applications, including wind, solar photovoltaic (PV), and electric vehicles [1], [2]. Consequently, the resulting electronic waste (E-waste) at the end of the service life of these renewable converters has become a significant concern [3]. Reducing E-waste and promoting Ecodesign for sustainable converter can be addressed through two main approaches: extending the service life of the converter and implementing effective end-of-life management, such as module reuse and material recycling [4]. Therefore, reliability-oriented design strategies are essential for minimizing the levelized cost of energy (LCOE) [5] and supporting sustainable renewable energy systems.

From the perspective of system-level reliability, the renewable power converter is the bottleneck as a large number of fragile elements are employed, such as semiconductors, capacitors, magnetics, controllers, sensors, etc [6]. The most fragile component of renewable power converters decides the lifetime of the entire electrical system, which is the famous barrel effect. As well known, the power converter module (combined with semiconductor devices) is one of the most vulnerable components in renewable power converters [7]. Unbalanced loss distribution of power devices will greatly increase the failure rate of a single semiconductor, which reduces the service life of the power converter module [8]. The unbalance temperature stresses are almost caused by asymmetric topology, the switching operation, and the bad forced cooling system [9].

Sustainable renewable energy converter Ecodesign seeks to reduce E-waste by extending the service life of power modules. The E-waste reduction can be achieved from two aspects: 1) Extending service life means delaying the elimination and reducing the average annual E-waste produced.; 2) The power module remains operational at the end of its originally designed system lifetime, allowing for recycling and reusing. Many solutions have been explored to deal with the unbalanced loss issue, where the research can be separated into two categories.

1) General lifetime enhanced methods: the general concept focuses on reducing the entire thermal stresses of power converters [10]. The widely used solution is to increase the volume of the heatsink [11] yet at the expense of power density and cost. Besides, the methods of decreasing switching frequency [12] and the reduction of operation power [13] come at the expense of power density, and energy utilization, respectively. The advanced method employs wide-band-gap devices instead of Si semiconductors [14]. The above solutions alleviate the temperature stresses overall with extra economic costs. Therefore, the reliability-oriented solutions directly addressing the unbalanced loss distribution problem may be much better.

2) Balanced solutions: the idea is to balance the thermal stresses of power devices through design and control. For instance, a good power device layout according to the cooling flowing way in the forced cooling system (e.g., the hottest component is set at the most effectively cooled position.) [15]. However, it is not suitable for outdoor power converters, which should meet the IP65 standard. The redundancy design is a promising way to share the thermal stresses of the hottest component, where the parallel structure (i.e., being hybrid structures mixed Si and SiC devices to have a better trade-off between efficiency and cost) shares the current stresses

Manuscript received Month xx, 2025; revised Month xx, xxxx; accepted Month x, xxxx. This work was supported by the Hong Kong Research Council Early Career Scheme under Grant 25238325

Y. Zhang and X. Zhang are with the Hong Kong Polytechnic University, Hong Kong; Z. Tang is with PV and Energy Storage Technology Platform Department, Sungrow Power Supply Co., Ltd, Hefei 230088, China. (emails: yiz@ieee.org, xy_zhang@ieee.org, tangzhongting@sungrowpower.com.)

© 2026 IEEE. Personal use of this material is permitted. Permission from IEEE must be obtained for all other uses, in any current or future media, including reprinting/republishing this material for advertising or promotional purposes, creating new collective works, for resale or redistribution to servers or lists, or reuse of any copyrighted component of this work in other works.

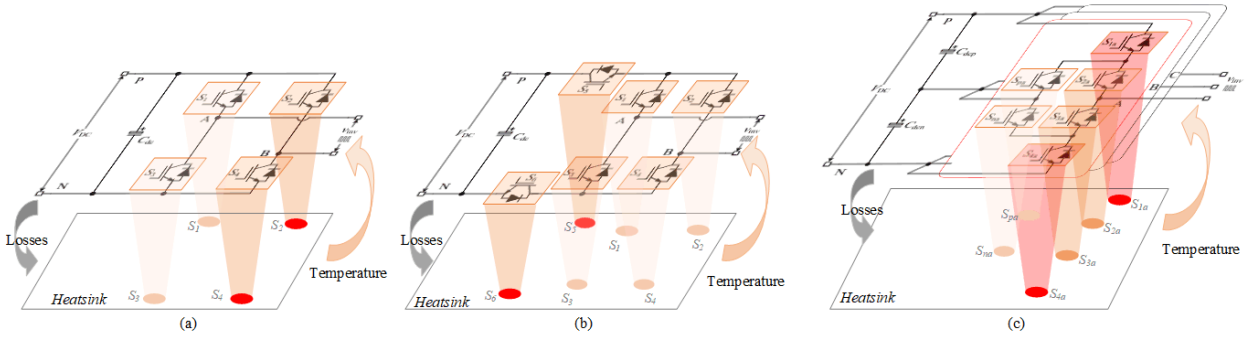

Fig. 1 Power loss distribution of typical renewable converter modules under the prior-art modulations. (a) Full-bridge inverter module. (b) DC-decoupling H6 inverter module. (c) ANPC converter module.

[16]–[18] and the cascade structure shares the voltage stresses [8], [19], [20], respectively. However, the unbalanced issue happens among the parallel and cascade switches due to the mismatched internal parameters of switches [8]. Moreover, an improved modulation method aims at the unbalanced loss issue in the active neutral-point-clamped (ANPC) converter due to its redundant commutations [21]. The idea is to distribute losses on average under the existing power converter module instead of adding extra costs. Although the balancing effect is limited by the power factor in the ANPC converter, this idea can be applied to virtually all converter modules with redundant operation capability [22], [23]. The improved modulation does not affect the performance of converters in areas such as output voltage, zero sequence, and current ripple.

Furthermore, the effect of unbalanced loss distribution on service life has not been comprehensively studied, and quantitative reliability assessments of power converter modules accounting for environmental and cooling conditions remain limited [24]. This paper addresses these gaps by investigating life-enhancing modulation techniques for unbalanced losses to support sustainable renewable converters. Section II analyzes the unbalanced loss distribution of a typical renewable converter module under traditional modulation, emphasizing the influence of power factor on loss distribution in full-bridge inverters. A life-enhancing modulation method that incorporates both online and offline state feedback is then proposed. Section III demonstrates loss distribution equalization using a full-bridge inverter module as an example. Section IV presents a comparative evaluation of electrical stress, thermal stress, and reliability based on Weibull distributions through annual mission profile experiments on a 5 kW system in Arizona [25], [26]. Section V evaluates the environmental impact of the proposed method using standard life cycle assessment (LCA) methodology. The paper concludes with a summary in Section VI.

II. Loss and Thermal Analysis

A. Loss distribution for typical renewable converters

As mentioned previously, the semiconductor is one of the fragile components of power converter modules, which plays a decisive role in the entire lifetime of the power converter. The power losses generated during the switching of semiconductors cause the rising of the junction temperature, which is critical in thermal fatigue degradation and lifetime prediction that are closely related to reliability evaluation [27]. There is no denying that the unbalanced power losses will cause uneven junction temperatures among semiconductors (i.e., resulting in different failure rates in a long-term operation), then reduce the service life of the power converter module. To thoroughly analyze the impact of the unbalanced loss distribution on the lifetime of the power converter module, the first step is to analyze the loss distribution in renewable converters under traditional modulations.

Fig. 1 shows the general power loss distribution for three typical renewable converter modules. Fig. 1(a) presents the loss distribution of the full-bridge inverter module under the traditional unipolar pulse width modulation (UPWM). The temperature of the two switches operated at a high frequency is higher than that of the other two switches under the fundamental frequency. For the DC-decoupling H6 inverter module in Fig. 1(b), the temperatures of the DC-decoupling switches S_5 and S_6 are higher than that of other rest switches [28]. That is because S_5 and S_6 are throughout operating at a high frequency. Besides, the total losses of the H6 module in Fig. 1(b) are higher than that of the full-bridge module in Fig. 1(a). Moreover, Fig. 1(c) shows the ANPC converter module, which is preferred in the renewable power converters [29]. The ANPC module has an inherent thermal unbalance among devices of the same phase under the traditional modulation methods [30]. As shown in Fig. 1(c), due to the different utilization of the devices in multilevel voltage outputs, the upper and lower switches are warmer than the middle two switches in one phase, and the active clamped switches are the coolest ones.

Hereby, to validate the lifetime enhancement performance of the proposed method, the full-bridge inverter module is detailed in the thermal stress analysis and the lifetime evaluation under both the traditional and proposed modulation methods.

B. Thermal stress of the full-bridge inverter module with traditional UPWM

The full-bridge inverter module in Fig. 1 (a) has four switches of Insulated Gate Bipolar Transistors (IGBT) $S_{1\text{-}4}$

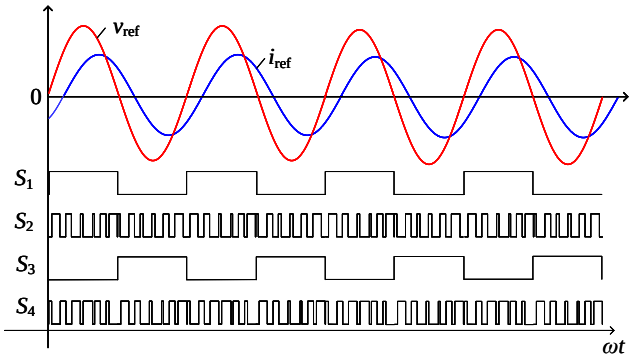

Fig. 2 Traditional UPWM method for the full-bridge inverter module with reactive power injection.

(with the anti-paralleled diodes $D_{1\text{-}4}$). And C_{dc} represents the DC-link capacitor, V_{dc} is the DC-link voltage, and v_{inv} is the modulated output voltage. To achieve reactive power injection and high efficiency, the traditional UPWM operates two switches (i.e., S_1, S_3) at the fundamental frequency and the other two switches (i.e., S_2, S_4) are at a high-frequency transition, as demonstrated in Fig. 2. In addition, v_{ref} and i_{ref} are the reference voltage and current.

Power losses of semiconductor devices [31] include switching losses P_{sw} and conduction losses P_C, respectively. Among them, switching losses P_{sw} can be expressed as

$$P_{sw} = P_{swT} + P_{swD} = (E_{onT} + E_{offT} + E_{onD}) f_{sw} \frac{V_{ceav} I_{cav}}{V_{CC} I_{CC}} \quad (1)$$

where P_{swT} and P_{swD} are switching losses of the IGBT and the anti-parallel diode, respectively. f_{sw} is the switching frequency. E_{onT}, E_{offT}, and E_{onD} are the turn-ON, turn-OFF, and diode reverse-recovery energy, respectively, which are provided in the datasheet under certain test conditions (i.e., the test collector-emitter voltage V_{CC} and the test collector current I_{CC}). Besides, V_{ceav} and I_{cav} are the average collector-emitter voltage and the average collector current of power devices operating in the converter module.

According to Eq. (1), switching losses are mainly distributed at S_2 and S_4, as shown in Fig. 3(a). When considering conduction losses are equal in each power device, the unbalanced power losses can be compared in Table II. Since the fundamental frequency f_g is far less than the high switching frequency f_{hf} (being above kHz level), the switching losses of S_1 and S_3 can be neglected.

When considering the impact of reactive power injection, conduction losses P_C are composed of conduction losses in IGBTs (P_{CT}) and diodes (P_{CD}), which can be calculated as

$$P_{CT} = \frac{1}{\pi} \int_0^{\varphi+\pi} \frac{V_m \cos\omega t}{V_{dc}} (V_{ce0} + r_c I_m \cos(\omega t + \varphi)) I_m \cos(\omega t + \varphi) d\omega t \quad (2)$$

$$P_{CD} = \frac{1}{\pi} \int_0^{\varphi+\pi} \frac{V_m \cos\omega t}{V_{dc}} (V_{d0} + r_d I_m \cos(\omega t + \varphi)) I_m \cos(\omega t + \varphi) d\omega t \quad (3)$$

where V_{ce0}, r_c, V_{d0} and r_d are the IGBT on-state zero-current collector-emitter voltage, the collector-emitter on-state resistance, the diode on-state zero-current voltage and the diode on-state resistance, respectively. φ is the power factor angle, V_m and I_m are the amplitude of the AC output voltage and current, respectively. ω is the fundamental angular frequency.

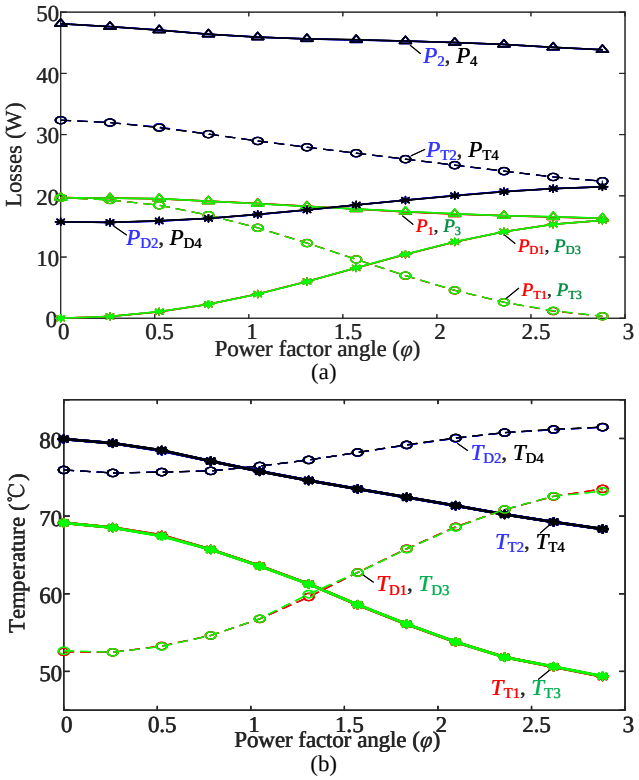

Fig. 3 Thermal stress analysis of IGBTs (FS25R12KT3) in the 5 kW full-bridge inverter module under different power factors. (a) Power loss distribution. (b) Thermal performance.

Therefore, conduction losses of the full-bridge module are mainly distributed among IGBTs when generating positive apparent power, while the losses are distributed among body diodes for generating negative apparent power. Eqs. (2) and (3) imply that conduction losses are unbalanced between IGBTs and diodes with different power factor angles, as presented in Fig. 3(a) and (b). Moreover, the thermal stress of IGBTs under the ambient temperature of 25 °C is presented in Fig. 3 (b). The temperatures of anti-parallel diodes and IGBTs change along with the power factor, where the higher the power factor is, the higher temperatures of diodes $D_{1,3}$ are and the lower temperatures of $T_{1,3}$ are. However, the temperature of both anti-parallel diodes and IGBTs in $S_{2,4}$ are always higher than that in $S_{1,3}$.

Since each semiconductor device integrates a IGBT and an anti-parallel diode, the total power losses $P_{1\text{-}4}$ are considered in the lifetime analysis. From the perspective of the entire semiconductor device, the unbalanced issue of the full-bridge module [22] is mainly caused by switching losses. The unbalanced issue of the DC-decoupling H6 inverter module (Fig. 1 (b)) happened due to unbalanced conduction losses [9]. The unbalanced problem in the ANPC inverter module (Fig. 1 (c)) is impacted by both unbalanced conduction losses and reactive power injection [32].

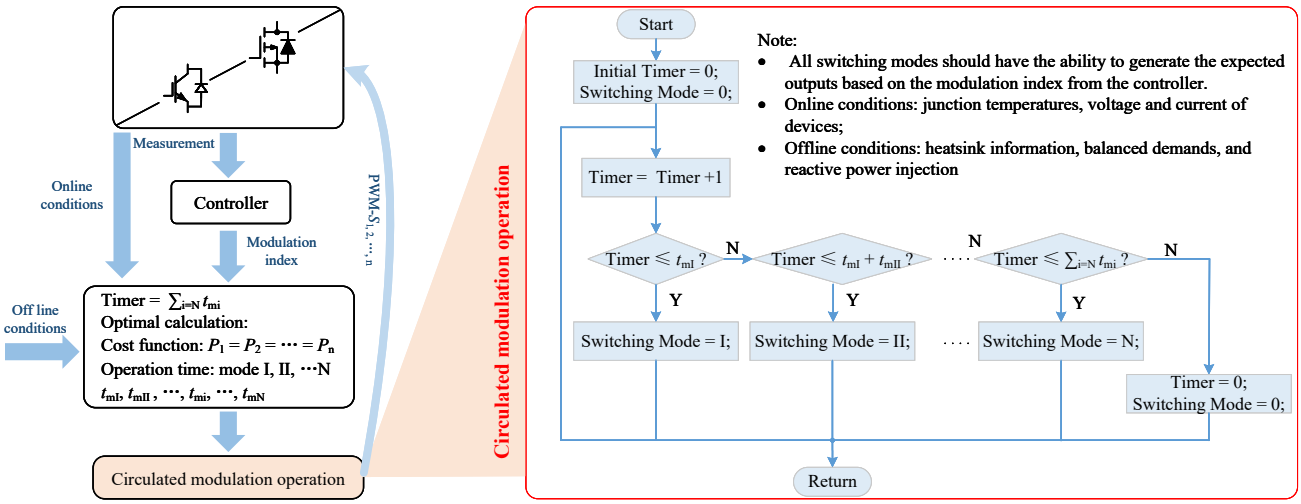

Fig. 4 Proposed generalized lifetime enhanced modulation method.

III. Proposed Lifetime Enhanced Modulation Method

A. Generalized Lifetime Enhanced Modulation Method

Based on the above analysis, the unbalanced loss issues of power devices are mainly caused by the different switching frequencies, unbalanced conduction losses, reactive power injection, and so on. To achieve a comprehensive balanced solution, a lifetime enhanced modulation method has been proposed, as shown in Fig. 4. The proposed method defines operating times $t_{\text{mI, mII, ..., mN}}$ for corresponding switching modes (I, II, ..., N) to ensure the loss balance. These operating times $t_{\text{mI, mII, ..., mN}}$ can be determined based on temperature information obtained through either online condition monitoring or offline condition analysis: 1) *Online condition monitoring*, the junction temperature is measured using an additional temperature sensor. However, this approach exhibits hysteresis, which may degrade balancing performance. 2) *Offline condition analysis*, this method relies on thermal distribution simulations of the power module in practical applications to derive temperature information. It offers lower cost and higher reliability for lifetime enhancement compared to online monitoring. Therefore, this study adopts the offline method for analysis. The average power loss of each switch under different operating modes can be expressed as

$$\begin{cases} P_1 = \dfrac{P_{\text{I1}}t_{\text{mI}} + P_{\text{II1}}t_{\text{mII}} + \ldots + P_{\text{N1}}t_{\text{mN}}}{\sum_{\text{i=N}} t_{\text{mi}}} \\ P_2 = \dfrac{P_{\text{I2}}t_{\text{mI}} + P_{\text{II2}}t_{\text{mII}} + \ldots + P_{\text{N2}}t_{\text{mN}}}{\sum_{\text{i=N}} t_{\text{mi}}} \\ \ldots \\ P_{\text{n}} = \dfrac{P_{\text{In}}t_{\text{mI}} + P_{\text{IIn}}t_{\text{mII}} + \ldots + P_{\text{Nn}}t_{\text{mN}}}{\sum_{\text{i=N}} t_{\text{mi}}} \end{cases} \tag{4}$$

During operation, thermal simulations are first conducted to determine the thermal impedance of each switch within the power module, denoted as Z_{th1}, Z_{th2}, ..., Z_{thn}. By combining the calculated power losses with the corresponding thermal impedances, the junction temperature rise of each switch can be estimated. To ensure thermal balance, the objective function is formulated as

$$P_1 Z_{\text{th1}} = P_2 Z_{\text{th2}} = \ldots = P_{\text{n}} Z_{\text{thn}} \tag{5}$$

By solving Eqs. (4) and (5), the corresponding operating times $t_{\text{mI, mII,..., mN}}$ can be determined. Since junction temperature estimation involves complex convolution operations, Eq. (5) simplifies the process by considering only the thermal resistance R_{th} instead of the thermal impedance Z_{th}. The operation mode is updated periodically, where the circulation timer = $\sum_{\text{i=N}} t_{\text{mi}}$ is set to a multiple of N/f_{g}, with the circulated scheme detailed in Table I. Implementation of the proposed method requires a timer function and a mode-selection function. Both functions involve only integer operations, imposing minimal computational load on the microprocessor.

TABLE I Process of the proposed circulated scheme

Algorithm 1 Circulated modulation control scheme

Input Operation time $t_{\text{mi}}, i = I, II, ..., N$ of each operation mode.
Output Select the switching mode for the current operation.
1: Initial Timer = 0 and Switching Mode = 0.
2: Timer starts timing: Timer = Timer+1.
3: Switching Mode Selection
  If Timer $\leq t_{\text{mI}}$
    Switching Mode = I.
  Else if Timer $\leq t_{\text{mI}} + t_{\text{mII}}$
    Switching Mode = II.
    ...
  Else if Timer $\leq \sum_{\text{i=N}} t_{\text{mi}}$
    Switching Mode = N.
  Else
    Timer = 0;
    Switching Mode = 0;
  end
4: Timer stops, parameter resets, and return to the next circle.

TABLE II Loss comparison of power devices in the full-bridge inverter module

Switches	Loss model
S_1, S_3	$P_{\mathrm{C}} + (E_{\mathrm{onT}} + E_{\mathrm{offT}} + E_{\mathrm{onD}}) f_{\mathrm{g}} \frac{2V_{\mathrm{dc}} I_{\mathrm{m}}}{\pi V_{\mathrm{CC}} I_{\mathrm{CC}}}$
S_2, S_4	$P_{\mathrm{C}} + (E_{\mathrm{onT}} + E_{\mathrm{offT}} + E_{\mathrm{onD}}) f_{\mathrm{hf}} \frac{2V_{\mathrm{dc}} I_{\mathrm{m}}}{\pi V_{\mathrm{CC}} I_{\mathrm{CC}}}$

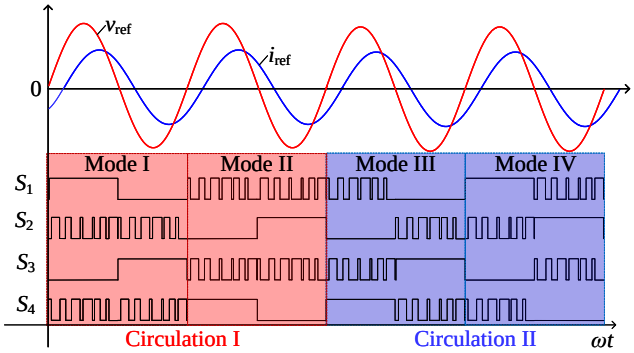

Fig. 5 Switching modes and circulation ways of the full-bridge inverter module.

B. Case Study in the Full-bridge Inverter Module

The proposed lifetime enhanced modulation method has been specified in the full-bridge inverter module. As shown in Table III, there are four operation states of the full-bridge inverter to enable reactive power injection, where '↑↓' represents complementary switch instants at a high switching frequency. When $v_{\mathrm{ref}} > 0$, the full-bridge inverter operates at both states **A** and **C**, generating a positive voltage $+v_{\mathrm{inv}}$. While $v_{\mathrm{ref}} < 0$, it operates at states **B** and **D** to generate a negative voltage $-v_{\mathrm{inv}}$. The four operation states are combined into four switching modes for the DC-AC conversion, i.e., Mode I – states **A** and **B**, Mode II – states **C** and **D**, Mode III – states **A** and **D** and Mode IV – states **B** and **C**. The four switching modes are shown in Fig. 5. The traditional UPWM in Fig. 2 only adopts Mode I, leading to the unbalanced loss issue.

As shown in Fig. 5, the proposed lifetime enhanced modulation method for the full-bridge module changes the switching mode cyclically at a low frequency (i.e., the timer is equal to $2/f_{\mathrm{g}}$). It should be noted that the circulation time should be selected reasonably to avoid large fluctuations of the junction temperature in power devices, which is revealed in [25] that the constant junction temperature benefits the power device's lifetime. There are two examples of the proposed circulation switching method detailed in Fig. 5, i.e., Circulation I – Mode I + Mode II, and Circulation II – Mode III + Mode IV. Besides, the full-bridge module performs two different switching modes alternatively for each circulated time.

The corresponding thermal stresses analysis of IGBTs in the full-bridge inverter module with the proposed method are shown in Fig. 6, where Fig. 6(a) presents power loss distribution performance and Fig. 6(b) is the temperature performance of IGBTs and anti-parallel diodes. It can be revealed in Fig. 6(a) that power losses on IGBTs $P_{\mathrm{T1\text{-}T4}}$ and diodes $P_{\mathrm{D1\text{-}D4}}$ are equal respectively. Although the distributed losses of the

TABLE III Operation states of the full-bridge Inverter.

Operation states	Periods	S_1	S_2	S_3	S_4
A	$v_{\mathrm{ref}} > 0$	ON	↑↓	OFF	↑↓
B	$v_{\mathrm{ref}} < 0$	OFF	↑↓	ON	↑↓
C	$v_{\mathrm{ref}} > 0$	↑↓	OFF	ON	↑↓
D	$v_{\mathrm{ref}} < 0$	↑↓	ON	OFF	↑↓

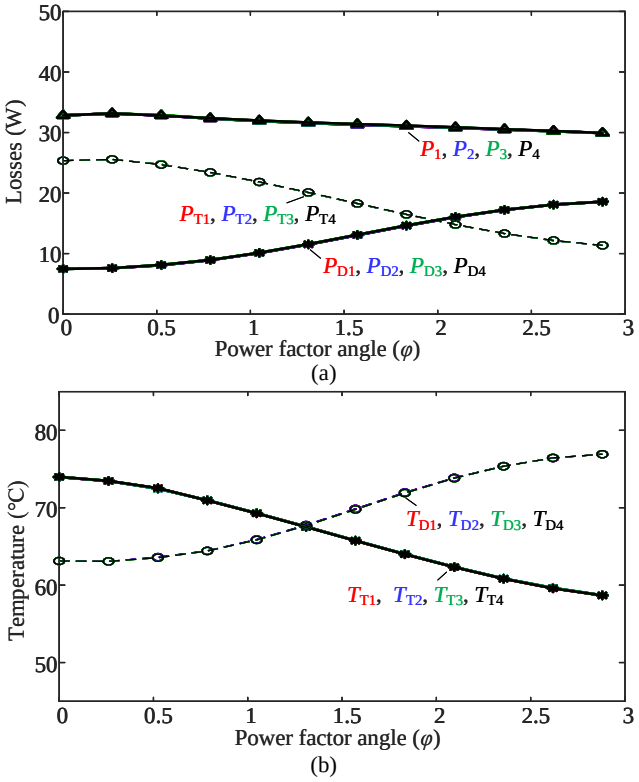

Fig. 6 Thermal stress analysis of IGBTs in a 5 kW full-bridge inverter module with the proposed lifetime enhanced modulation method. (a) Power loss distribution. (b) Thermal performance for each switch.

single semiconductor die (IGBTs and diodes) vary with power factor, the total power losses of each device $P_{\mathrm{1\text{-}4}}$ are equal. This preliminary validation demonstrates that the proposed modulation method effectively balances power losses in the full-bridge inverter module. In addition, compared with Fig. 3, the overall module losses remain nearly unchanged, indicating that the proposed method does not alter the operation of the system. As shown in Fig. 6(b), at an ambient temperature of 25 °C, the thermal stresses of the IGBTs and diodes are nearly identical. While variations in power factor influence the thermal stress of each device type, the total thermal stress per device remains essentially equivalent. These results further confirm the effectiveness of the proposed modulation method in balancing the average thermal stress of semiconductor devices in the full-bridge inverter module.

Consequently, the proposed method can ensure the full-bridge module has a balanced power loss distribution, allowing a longer service life and facilitating reusing and recycling. Compared to adding extra power components, the proposed

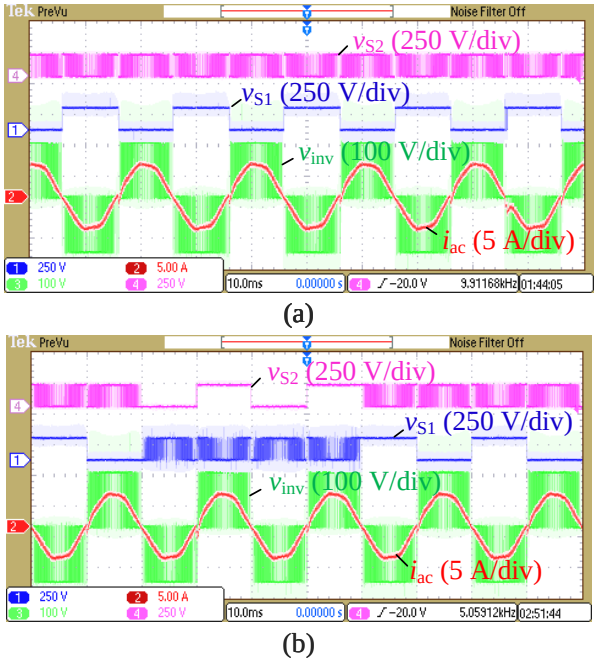

Fig. 7 Electric stress performance comparison for the full-bridge inverter module. (a) With the traditional UPWM. (b) With the proposed lifetime enhanced modulation method.

modulation method slightly increases calculation burdens, while achieving relatively high cost-effectiveness.

IV. Experiments and Validations

A. Experimental Results

Experiments are carried out on a full-bridge inverter module, where V_{dc} is 250 V, v_{ac} is 110 V / 50 Hz (RMS), and the switching frequency f_{sw} is 20 kHz. The DC input adopts a DC power supply, and the AC output employs a resistor load. The power factor here is 1.

Fig. 7 compares the electric stress performance of the full-bridge module under the traditional UPWM and the proposed modulation methods. The nomenclature includes: v_{S1} and v_{S2} are the voltage of semiconductors S_1 and S_2, v_{inv} and i_{ac} represent the inverter differential voltage and the output current. As shown in Fig. 7(a), v_{S1} changes at the grid frequency (50 Hz), and v_{S2} changes at a high switching frequency (20 kHz). The pulse performance agrees well with the traditional UPWM in Fig. 2. In contrast, the switching frequencies of v_{S1} and v_{S2} change alternatively with the proposed modulation method of the cyclic switching mode, as presented in Fig. 7(b). The circulated time is 40 ms, i.e., two times the grid fundamental cycle (20 ms). The results suggest that the proposed modulation method can ensure the same electric stresses of the full-bridge inverter module, balancing the power losses.

Before the thermal stress comparison, the bird view of the full-bridge inverter module is exhibited in Fig. 8(a), which is FS50R12KT4-B15 from Infineon Technologies. Two phase legs of a three-phase IGBT power module are considered for better comparison considering the good consistency of switches on one module. As shown in Fig. 8(a), the left

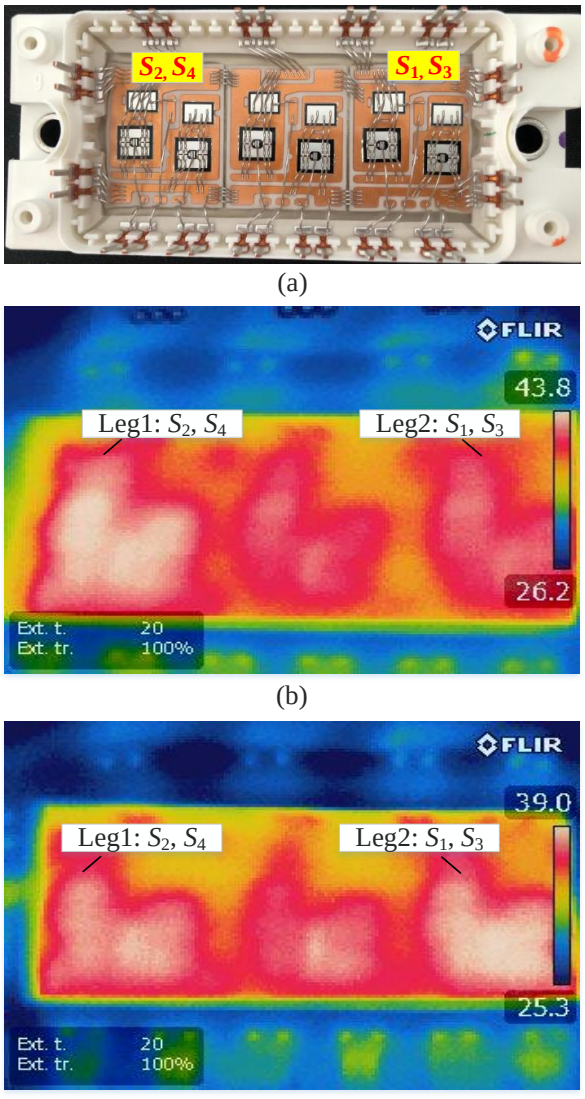

Fig. 8 Thermal stress performance comparison for the full-bridge inverter module. (a) Bird-view of the semiconductor module. (b) With the traditional UPWM. (c) With the proposed lifetime enhanced modulation method.

phase-leg are devices of S_2 and S_4, and the right phase-leg are devices of S_1 and S_3. Then, the thermal stresses have been compared between the traditional UPWM and the proposed method in the following two subfigures. As shown in Fig. 8 (b), the temperatures of $S_{2,4}$ are higher than those of $S_{1,3}$ when the inverter is employing the traditional UPWM method. The temperatures of $S_{1\text{-}4}$ are almost identical with the proposed modulation method, as demonstrated in Fig. 8(c). Besides, the highest temperature in Fig. 8(b) (i.e., adopting the traditional UPWM) is 43.8 °C, which is higher than that (39 °C) in Fig. 8(c) (i.e., adopting the proposed UPWM method). It can be verified in Fig. 8 that the proposed lifetime enhanced modulation method can address the loss unbalance issue, achieving identical junction temperature of the power switches.

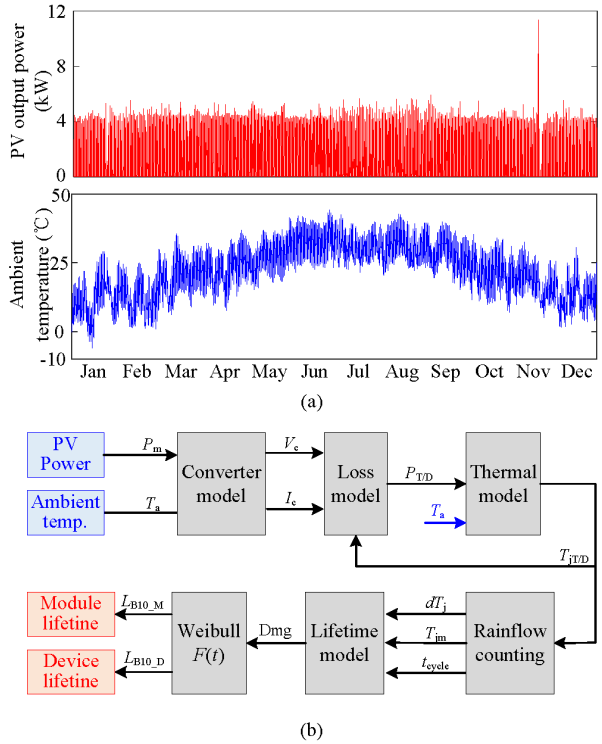

Fig. 9 Lifetime estimation inputs. (a) Annual mission profile of the output power and ambient temperature from a 5 kW PV system (Arizona, US) with a sample rate of 1 second. (b) Flow chart of lifetime estimation.

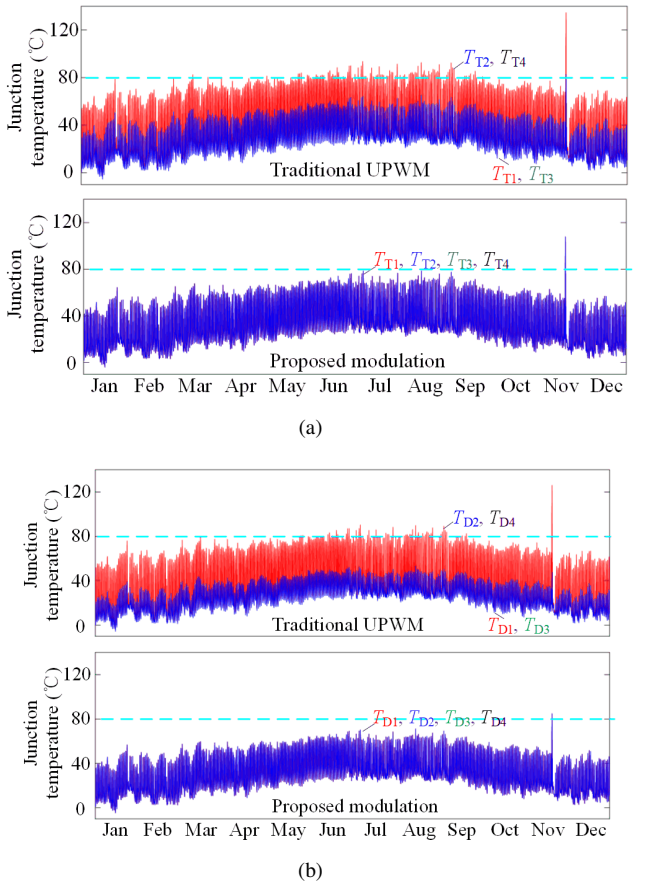

Fig. 10 Annual profiles of semiconductor devices in the full-bridge inverter under different modulations, (a) IGBT Thermal profiles and (b) Anti-parallel diodes thermal profiles.

B. Reliability Validations

To validate the reliability increase, a PV system case, and the lifetime estimation procedure are introduced in Fig. 9. Fig. 9 (a) is an annual PV output power and ambient temperature sampled every second. The annual mission profile is from a 5 kW PV power generator located in Arizona, US. The lifetime estimating procedure is introduced in Fig. 9 (b) [26], which can be detailed in the following.

1) The voltage and current can be calculated through the full-bridge inverter module and the annual mission profile of the PV output power;

2) With the converter voltage and current mission profile, the power losses of IGBTs and anti-parallel diodes can be achieved through the losses model, which is built based on Eqs. (1)-(3).

3) The thermal model of the full-bridge inverter module is built to evaluate the annual thermal profile of the semiconductor devices, including the annual temperature profile of IGBTs and anti-parallel diodes.

4) According to the above outcome, the Coffin-Manson lifetime model is combined with Monte Carlo simulation to account for environmental and parameter uncertainties. This approach enables the derivation of the Weibull distribution and the determination of the B_{10} lifetime for both individual devices and the overall inverter module [33], [34].

According to the procedure, the annual thermal stresses of IGBTs and anti-parallel diodes have been compared between the traditional UPWM and the proposed modulation, as shown in Fig. 10 (a) and (b), which are the thermal performance of IGBTs and diodes, respectively. The annual thermal profiles indicate that the thermal stresses are unbalanced in both IGBTs and diodes of the full-bridge inverter module with the traditional UPWM. While, the proposed modulation method can ensure average temperatures in both.

Moreover, the unreliability curve with the operation year is compared through the rainflow counting and the lifetime model, in which Fig. 11 (a) and (b) are the unreliability of the full-bridge inverter under the traditional UPWM and the proposed modulation, respectively. In the case of the series connection in the reliability block diagram in [34], the converter reliability function is the production of each semiconductor device's reliability. Fig. 11 (a) shows that the B_{10} lifetime of the full-bridge inverter is 11.5 years when adopting the traditional UPWM, while that in Fig. 11 (b) is 116 years when adopting the proposed modulation (i.e., being 10 times lifetime increasing).

In a word, the proposed lifetime enhanced modulation can balance the power losses, ensure even thermal stresses, and increase the full-bridge inverter reliability greatly. This level of lifetime improvement promotes the reuse of power converter modules and reduces the E-waste. Besides, the proposed modulation concept can be extended to other renewable converter modules, such as the mentioned DC-decoupling H6 inverter

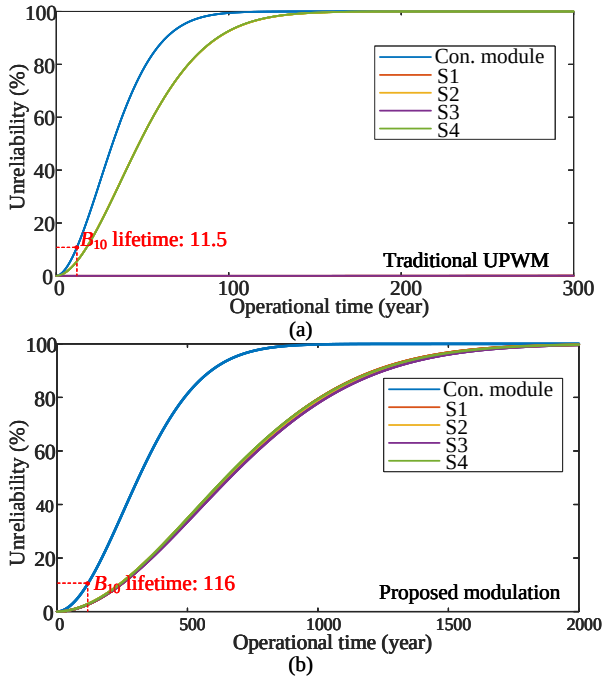

Fig. 11 Unreliability curve from a single device to the entire full-bridge inverter module under different modulation methods. (a) With the traditional UPWM. (b) With the proposed lifetime enhanced modulation method.

(Fig. 1 (b)) and ANPC converter (Fig. 1 (c)).

V. Environmental Impact Assessment of Power Modules

LCA is a widely recognized and internationally standardized method for quantifying the environmental impact of power modules over their entire life cycle. To further validate the effectiveness of the proposed method, this paper compares the carbon footprint of power modules under two different modulation strategies using LCA.

A. Life Cycle Assessment Process

The scope of LCA covers the entire process from raw material extraction to product recycling or disposal. For power modules, the life cycle is structured into four stages, namely manufacturing, transportation, use, and end-of-life disposal [35]. As illustrated in Fig. 12, the environmental impact at each stage is systematically evaluated using the corresponding bill of materials.

1) Manufacture stage: The bill of materials was established, and corresponding processes, including raw material extraction, component production, and assembly, were modeled.

2) Transportation stage: Transport activities across the life cycle were included, considering both shipping and trucking, with distances and modes selected according to typical supply chain practices.

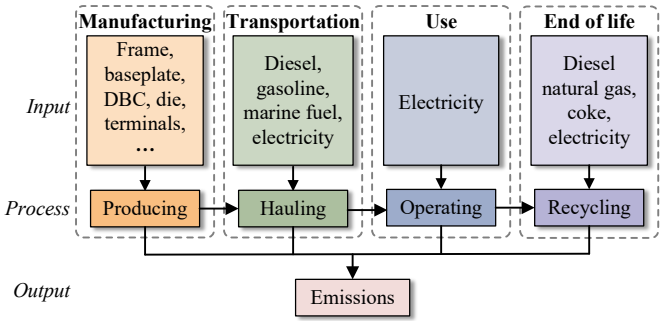

Fig. 12 Process of LCA for power modules.

3) Use stage: Energy consumption during the operational lifetime was calculated. The service life of the module was defined by the B10 lifetime (see Section IV), and corresponding energy consumption was quantified using Eqs. (1)-(3).

4) End-of-life: Disposal scenarios were modeled, including landfilling, incineration, and metal recycling, in line with common e-waste practices.

Publicly available data for commercial power modules suitable for detailed LCA is limited. However, prior studies on the life cycle assessment of power semiconductors provide relevant reference data, and part of the dataset used in this work is derived from the literature [35]–[37]. The assessment was carried out using the open-source platform OpenLCA, while life cycle inventory (LCI) data and process-specific datasets were obtained from the Ecoinvent database.

B. Life Cycle Assessment Results

During the LCA, the service life of photovoltaic inverters was set to 25 years. Fig. 14 presents the evolution of mineral and resource depletion (MRD) impacts over time under both modulation methods. As shown in Fig. 11, the B10 lifetime of power modules under traditional UPWM method is approximately 11.5 years. Consequently, replacements due to wear-out failures are required within the 25-year service life, resulting in additional manufacturing, transportation, and end-of-life disposal emissions. By contrast, the proposed method extends the module lifetime and avoids replacements within the same cycle. Since the Weibull distribution of power module reliability was obtained from 5,000 Monte Carlo simulations, Figure 14 also reports MRD results with 50% and 90% confidence intervals.

Additionally, Table IV summarizes the performance of power modules under the two methods. As the proposed approach does not compromise the converter's output capability, the total power dissipation remains nearly identical to that of traditional UPWM method. Nevertheless, the improved method achieves temperature equalization across the modules, thereby extending their operational lifetime. Over a 25-year service cycle, the proposed method ensures reliable operation without requiring replacement due to wear-out failures. In contrast, the traditional UPWM method, owing to unbalanced thermal stress distribution and accelerated degradation, necessitates two replacements within the same period. From a sustainability standpoint, the proposed method mitigates

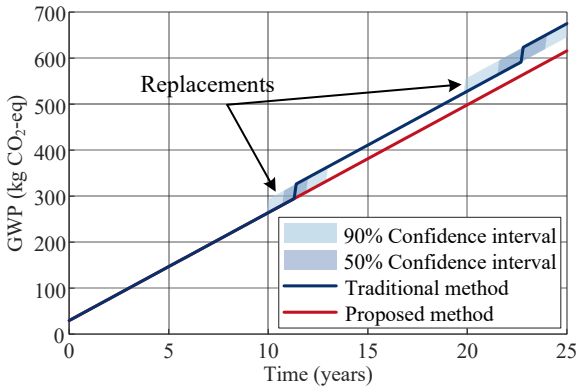

Fig. 13 Comparison of global warming potential (GWP) for the power modules under the proposed method and traditional method.

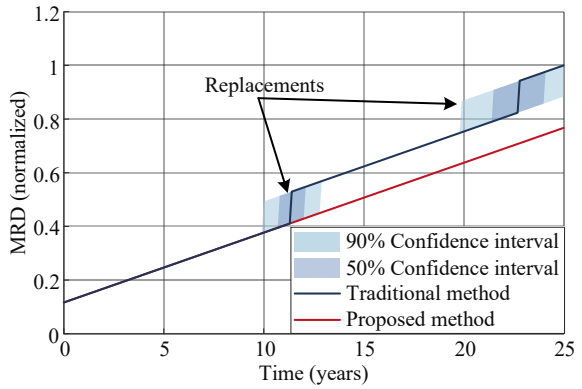

Fig. 14 Comparison of mineral and metal resource depletion (MRD) for the power modules under the proposed method and traditional method.

TABLE IV Comparison of the environmental impacts for the power modules over a 25-year service life using the proposed method and the traditional method.

Factors	Traditional method	Proposed method	Relative difference
Energy consumption per year /kWh	267.51	269.47	0.73%
B10 lifetime /years	11.5	116	908%
Global warming potential (GWP) /CO_2-eq	675	615	-8.89%
Mineral and metal resource depletion (MRD) /kg Sb-eq	0.0423	0.0324	-23.4%

environmental impact across life cycle stages, including raw material extraction, manufacturing, transportation and end-of-life treatment, by prolonging operational lifetime.

VI. Conclusion

In this paper, the lifetime enhanced modulation concept is proposed for sustainable renewable converters. The loss unbalance issue has been analyzed for three typical renewable converter modules, the full-bridge module, the DC-decoupling H6 module, and the ANPC module. Then, the full-bridge inverter module is exemplified to engage in the analysis of power loss distribution, thermal stresses, and lifetime performance under the traditional UPWM and the proposed modulation. The proposed lifetime enhanced modulation changes switching commutations cyclically based on offline or online conditions. The comparison between the traditional modulation and the proposed method has been performed through simulations, experiments, and reliability estimation. The results validate the proposed method can efficiently balance the losses of critical power switches and enhance the reliability of renewable converters without compromising system power density and cost. Furthermore, LCA results show that the proposed method avoids at least two device replacements over the service period, thereby reducing environmental impact. This highlights its significance for promoting sustainable renewable energy converter Ecodesign.

References

[1] F. Blaabjerg, Y. Yang, K. A. Kim, and J. Rodriguez, "Power electronics technology for large-scale renewable energy generation," *Proc. IEEE*, vol. 111, no. 4, pp. 335–355, 2023.

[2] Z. Tang, Y. Yang, and F. Blaabjerg, "Power electronics: The enabling technology for renewable energy integration," *CSEE Journal of Power and Energy Systems*, vol. 8, no. 1, pp. 39–52, 2022.

[3] C. P. B. et al., "The global e-waste monitor 2024: Treatment technology innovations." *Online*, 2024.

[4] A. Sangwongwanich, D.-I. Stroe, C. Mi, and F. Blaabjerg, "Sustainability of power electronics and batteries: A circular economy approach," *IEEE Power Electronics Magazine*, vol. 11, no. 1, pp. 39–46, 2024.

[5] J. Falck, C. Felgemacher, A. Rojko, M. Liserre, and P. Zacharias, "Reliability of power electronic systems: An industry perspective," *IEEE Industrial Electronics Magazine*, vol. 12, no. 2, pp. 24–35, 2018.

[6] H. Wang and F. Blaabjerg, "Power electronics reliability: State of the art and outlook," *IEEE Journal of Emerging and Selected Topics in Power Electronics*, vol. 9, no. 6, pp. 6476–6493, 2021.

[7] Y. Zhang, H. Wang, Z. Wang, Y. Yang, and F. Blaabjerg, "Impact of lifetime model selections on the reliability prediction of IGBT modules in modular multilevel converters," in *2017 IEEE Energy Conversion Congress and Exposition (ECCE)*, pp. 4202–4207, 2017.

[8] Z. Wang, H. Wang, Y. Zhang, and F. Blaabjerg, "Balanced conduction loss distribution among SMs in modular multilevel converters," in *2018 International Power Electronics Conference (IPEC-Niigata 2018 -ECCE Asia)*, pp. 3123–3128, 2018.

[9] "Energy efficiency enhancement in full-bridge PV inverters with advanced modulations," *e-Prime - Advances in Electrical Engineering, Electronics and Energy*, vol. 1, p. 100004, 2021.

[10] Z. Ni, X. Lyu, O. P. Yadav, B. N. Singh, S. Zheng, and D. Cao, "Overview of real-time lifetime prediction and extension for SiC power converters," *IEEE Transactions on Power Electronics*, vol. 35, no. 8, pp. 7765–7794, 2020.

[11] H. Jia, J. Chen, H. Fu, R. Qiu, and Z. Liu, "Intelligent prediction method for heat dissipation state of converter heatsink," *IEEE Access*, vol. 11, pp. 19 103–19 110, 2023.

[12] L. Wei, J. McGuire, and R. A. Lukaszewski, "Analysis of PWM frequency control to improve the lifetime of PWM inverter," *IEEE Transactions on Industry Applications*, vol. 47, no. 2, pp. 922–929, 2011.

[13] M. Andresen, G. Buticchi, and M. Liserre, "Thermal stress analysis and MPPT optimization of photovoltaic systems," *IEEE Transactions on Industrial Electronics*, vol. 63, no. 8, pp. 4889–4898, 2016.

[14] H. Beiranvand, E. Rokrok, and M. Liserre, "Comparative study of heatsink volume and weight optimization in SST DAB cells employing GaN, SiC-MOSFET and Si-IGBT switches," in *2019 10th International Power Electronics, Drive Systems and Technologies Conference (PEDSTC)*, pp. 297–302, 2019.

[15] U.-M. Choi, I. Vernica, and F. Blaabjerg, "Effect of asymmetric layout of IGBT modules on reliability of motor drive inverters," *IEEE Transactions on Power Electronics*, vol. 34, no. 2, pp. 1765–1772, 2019.

[16] A. H. Ranjbar, B. Abdi, and O. MahinFallah, "Effect of paralleling switches on reduction of reliability of fuel cell DC-DC converters," in *2008 Twenty-Third Annual IEEE Applied Power Electronics Conference and Exposition*, pp. 304–308, 2008.

[17] A. Deshpande and F. Luo, "Practical design considerations for a Si IGBT + SiC MOSFET hybrid switch: Parasitic interconnect influences, cost, and current ratio optimization," *IEEE Transactions on Power Electronics*, vol. 34, no. 1, pp. 724–737, 2019.
[18] P. Ning, T. Yuan, Y. Kang, C. Han, and L. Li, "Review of Si IGBT and SiC MOSFET based on hybrid switch," *Chinese Journal of Electrical Engineering*, vol. 5, no. 3, pp. 20–29, 2019.
[19] A. Lashab, D. Sera, F. Hahn, L. Camurca, Y. Terriche, M. Liserre, and J. M. Guerrero, "Cascaded multilevel PV inverter with improved harmonic performance during power imbalance between power cells," *IEEE Transactions on Industry Applications*, vol. 56, no. 3, pp. 2788–2798, 2020.
[20] J. Guo, X. Wang, J. Liang, H. Pang, and J. GonÃ§alves, "Reliability modeling and evaluation of MMCs under different redundancy schemes," *IEEE Transactions on Power Delivery*, vol. 33, no. 5, pp. 2087–2096, 2018.
[21] T. Bruckner, S. Bernet, and H. Guldner, "The active NPC converter and its loss-balancing control," *IEEE Transactions on Industrial Electronics*, vol. 52, no. 3, pp. 855–868, 2005.
[22] Z. Tang, Y. Yang, and F. Blaabjerg, "Loss unbalance issue of the full-bridge inverter with reactive power injection," in *2021 IEEE Applied Power Electronics Conference and Exposition (APEC)*, pp. 1451–1451, 2021.
[23] S. L.U., B. J., and T. S., "Hybrid PWM strategies for power balance in H bridge inverter," in *2014 International Conference on Computation of Power, Energy, Information and Communication (ICCPEIC)*, pp. 536–539, 2014.
[24] K. S. P. Kiranmai, R. V. Damodaran, M. Hushki, and H. Shareef, "An alternate hybrid PWM for uniform thermal sharing in single phase voltage-source inverter," *Sci Rep*, vol. 13, no. 1, p. 3348, Feb. 2023. [Online]. Available: https://www.nature.com/articles/s41598-023-30169-y
[25] Y. Zhang, H. Wang, Z. Wang, F. Blaabjerg, and M. Saeedifard, "Mission profile-based system-level reliability prediction method for modular multilevel converters," *IEEE Transactions on Power Electronics*, vol. 35, no. 7, pp. 6916–6930, 2020.
[26] D. Zhou and F. Blaabjerg, "Converter-level reliability of wind turbine with low sample rate mission profile," *IEEE Transactions on Industry Applications*, vol. 56, no. 3, pp. 2938–2944, 2020.
[27] H. Chen, J. Yang, and S. Xu, "Electrothermal-based junction temperature estimation model for converter of switched reluctance motor drive system," *IEEE Transactions on Industrial Electronics*, vol. 67, no. 2, pp. 874–883, 2020.
[28] A. Chanekar, N. Deshmukh, A. Gangwar, and S. Anand, "Thermal stress balancing for lifetime improvement of H6 solar inverter," in *2023 25th European Conference on Power Electronics and Applications (EPE'23 ECCE Europe)*, pp. 1–9, 2023.
[29] A. Nabae, I. Takahashi, and H. Akagi, "A new neutral-point-clamped PWM inverter," *IEEE Transactions on Industry Applications*, vol. IA-17, no. 5, pp. 518–523, 1981.
[30] M. Novak, V. Ferreira, M. Andresen, T. Dragicevic, F. Blaabjerg, and M. Liserre, "FS-MPC based thermal stress balancing and reliability analysis for NPC converters," *IEEE Open Journal of Power Electronics*, vol. 2, pp. 124–137, 2021.
[31] G. DuÅ¡an and P. Marco, "IGBT power losses calculation using the data-sheet parameters," *Germany: Infineon*, vol. 1st ed.,Neubiberg, pp. 5–6, 2009.
[32] J. Zaragoza, J. Pou, S. Ceballos, E. Robles, P. Ibanez, and J. L. Villate, "A comprehensive study of a hybrid modulation technique for the neutral-point-clamped converter," *IEEE Transactions on Industrial Electronics*, vol. 56, no. 2, pp. 294–304, 2009.
[33] P. Lall, M. Islam, M. Rahim, and J. Suhling, "Prognostics and health management of electronic packaging," *IEEE Transactions on Components and Packaging Technologies*, vol. 29, no. 3, pp. 666–677, 2006.
[34] D. Zhou, G. Zhang, and F. Blaabjerg, "Optimal selection of power converter in DFIG wind turbine with enhanced system-level reliability," *IEEE Transactions on Industry Applications*, vol. 54, no. 4, pp. 3637–3644, 2018.
[35] B. Baudais, H. Ben Ahmed, G. Jodin, N. Degrenne, and S. Lefebvre, "Life cycle assessment of a 150 kW electronic power inverter," *Energies*, vol. 16, no. 5, 02 2023.
[36] B. Baudais, N. Degrenne, H. B. Ahmed, G. Jodin, and S. Lefebvre, "PELCA: An open-source research power electronics life cycle assessment tool," in *PCIM Conference 2025; International Exhibition and Conference for Power Electronics, Intelligent Motion, Renewable Energy and Energy Management*, pp. 569–575, 2025.
[37] L. Fang, Y. Rosset, B. Sarrazin, P. Lefranc, and M. Rio, "Parametric LCA model for power electronic ecodesign process: Addressing MOSFET-Si and HEMT-GaN technological issues," *IET Power Electronics*, vol. 18, no. 1, p. e12844, 2025.

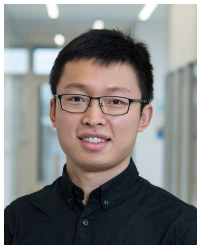

Yi Zhang (Senior Member, IEEE) received the B.S. and M.S. degrees from the Harbin Institute of Technology, Harbin, China, in 2014 and 2016, respectively, and the Ph.D. degree from Aalborg University, Aalborg, Denmark, in 2020, all in electrical engineering.

He is currently an Assistant Professor with the Hong Kong Polytechnic University, Hong Kong. During 2020–2023, he was affiliated with multiple institutions as a DFF International Postdoctoral Research Fellow, including RWTH Aachen University, Aachen, Germany, Swiss Federal Institute of Technology Lausanne, Lausanne, Switzerland, and Massachusetts Institute of Technology, Cambridge, MA, USA. He was also a Visiting Scholar with the Georgia Institute of Technology, Atlanta, GA, USA, in 2018. His research focuses on advancing the reliability and sustainability of power electronics through design, testing, packaging, and condition monitoring.

Dr. Zhang received the IEEE PELS Ph.D. Thesis Talk Award (2020), the First and Second Place Prize Paper Awards of IEEE TRANSACTIONS ON POWER ELECTRONICS (2021, 2025), and the Second Place Prize Paper Award of IEEE TRANSACTIONS ON INDUSTRY APPLICATIONS (2025).

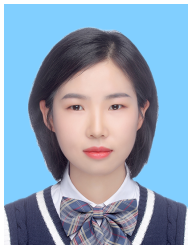

Xinyue Zhang (Member, IEEE) received the B.S. and M.S. degrees in 2016 and 2019, respectively, and the Ph.D degree in 2025, all in electrical engineering from Northwestern Polytechnical University, Xi'an, China. She was a visiting student at Aalborg University, Aalborg, Denmark, from 2022 to 2023. She is currently working as a postdoctoral fellow with the Hong Kong Polytechnic University, Hong Kong.

Her research interests include thermal analysis, reliability analysis, and optimization design of power electronic components and converters.

Zhongting Tang (S'18-M'20) received her B.S. degree in Automation Control in 2012 and Ph.D. degree in Control Science and Engineering in 2020 from Central South University, Changsha, China. During 2018–2020, she studied as a guest Ph.D. student at the AAU Energy in Aalborg University, Aalborg, Denmark. She worked as a postdoc at AAU Energy from 2020 2024. Then, she joined in Control in Hardware as an engineer at Vestas Wind Systems A/S, Aarhus, Denmark. Currently, she is a system director in PV and Energy Storage Technology Platform of Sungrow Power Supply Co., Hefei, China.

Her research focuses on the topology, modulation technology, and reliability of the grid-tied photovoltaics converter, closed-loop impedance modeling for generic power electronics converters considering the EMI performance, and power conversion on Wind turbines. She received the CSEE JPES Excellent Paper Award in 2023.